Control of Wind Turbines: Past, Present, and Future

Jason H. Laks, Lucy Y. Pao, and Alan D. Wright

Abstract—We review the objectives and techniques used in the control of horizontal axis wind turbines at the individual turbine level, where controls are applied to the turbine blade pitch and generator. The turbine system is modeled as a flexible structure operating in the presence of turbulent wind disturbances. Some overview of the various stages of turbine operation and control strategies used to maximize energy capture in below rated wind speeds is given, but emphasis is on control to alleviate loads when the turbine is operating at maximum power. After reviewing basic turbine control objectives, we provide an overview of the common basic linear control approaches and then describe more advanced control architectures and why they may provide significant advantages.

I. INTRODUCTION

Wind energy is currently the fastest-growing source of electricity in the world. Wind power investment worldwide is expected to expand three-fold in the next decade, from about $18 billion in 2006 to $60 billion in 2016 [1]. In the U.S., where wind currently only provides about 1% of the nation's electricity, wind has the potential to provide up to 20% of the nation's electricity without major changes to the nation's electricity distribution system. However, there are still many unsolved challenges in expanding wind power. In this paper, we will overview the standard controls as well as recently developed advanced controls for variable-speed, horizontal axis wind turbines. For a more general tutorial on wind turbines, see [2] and the references therein

It is becoming more common for modern turbines to provide individual pitch actuators at each blade so that the number of control inputs available to the system designer is increased above the traditional generator torque control. Pitch commands to individual actuators are depicted schematically in Fig. 1. In addition, force/moment sensing or accelerometers can be installed at each blade individually as well as on the nacelle and tower. These additional inputs and outputs combine with the fact that the turbine structural modes couple with the drive train and pitch actuation through torque and bending moments to make the wind turbine an inherently multi-input-multi-output (MIMO) system. Indeed, as turbine size increases and weight/cost considerations motivate accommodation of increased flexibility, it becomes more critical to take into account coupling between different structural modes and to utilize more sophisticated control methods to deal with these effects. Further, increased flexibility of turbine structures brings to the fore-front the task of mitigating damaging loads at the blade roots and the tower base.

Advanced control methods for addressing these issues have been investigated for well over a decade (e.g., [3,4] and additional references reported in [5]), but apparently most commercial systems are still implemented using multiple single-input-single-output (SISO) loops [5]. Fig. 1, for example, shows two different controllers for the generator and pitch control loops; if the pitch commands are identical and based only on the high speed shaft velocity ω, then this configuration comprises two SISO controllers operating independently of each other as in Fig. 2 (a). In contrast, advanced control approaches are distinguished by the hallmarks that plant uncertainty is explicitly accounted for in the design [6], a multi-input, multi-output (MIMO) controller is designed that accommodates coupling between loops [7] (Fig. 2 (b)), or a robust MIMO method is utilized [8]. Additionally, methods employing adaptive [9,10,11,12] or nonlinear techniques [13,14,15] have also been reported. Our intention here is to provide an overview of linear controller objectives and designs utilizing deterministic approaches applied to blade pitch and torque control. In addition, we will demonstrate how any feedback architecture can be augmented with a disturbance feedforward compensator utilizing wind measurements that may be available from novel technologies on the horizon.

This paper is organized as follows. Section II presents a linearized wind turbine model and the main wind turbine operating regions. We review the standard control methods used in the two main operating regions in Section III. In Section IV, we discuss the design of advanced controllers and focus on a region of wind turbine control where the control objectives are largely regulation and disturbance rejection. This control region provides a fairly well-defined venue for the comparison of several controller architectures. Our goal is to demonstrate and compare the design of SISO and relatively straightforward MIMO compensators. In Section V, we demonstrate the potential improvement that may be realized when a feedback system is augmented with disturbance feedforward of wind measurements. Finally, we

J. H. Laks is a PhD student in the Electrical and Computer Engineering Department at the University of Colorado, Boulder, CO 80309-0425 USA (email: jhlaks@colorado.edu).

L. Y. Pao is a Professor in the Electrical and Computer Engineering Department at the University of Colorado, Boulder, CO 80309-0425 USA (e-mail: pao@colorado.edu).

A. Wright is a Senior Engineer at the National Renewable Energy Laboratory, 1617 Cole Boulevard, Golden, CO 80401-3393 USA (e-mail: alan_wright@nrel.gov).
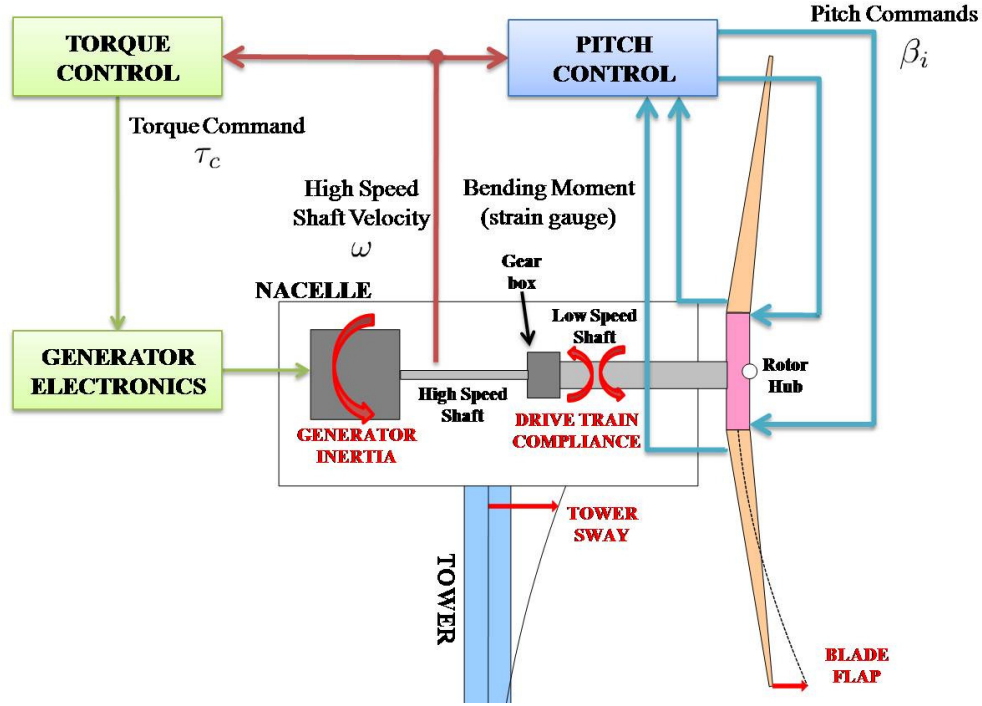
Fig. 1. Common turbine control loops. Generator speed is often the only measurement for both generator torque and pitch control. Supervisory control (not shown) can have additional measurements including local anemometer-based wind speed. More advanced turbines might also include individual blade bending moment/strain measurements and instrumentation for tower/nacelle accelerations.

close the paper by discussing ongoing and future challenges in Section VI.

II. REGIONS OF OPERATION AND LINEAR MODELS

In this section we characterize a linearized model of the turbine structural dynamics and view the generator as simply a static (unity) gain that translates commanded torque instantaneously into mechanical torque. There are many studies that focus on generator modeling and control and associated issues [6,13,14,16,17,18], but that is beyond the scope of this article where our focus is on pitch control and its effect on load mitigation and speed regulation.

A wind turbine is inherently nonlinear and time varying. Aerodynamic torques and bending moments depend nonlinearly on wind speed, pitch angle, and tower and blade deflections. Further, there is variation as the rotor turns to position the blades in a turbulent wind profile that varies spatially with respect to the rotor disk even in constant wind conditions. Nevertheless, good results have been obtained using linear, time invariant models of the turbine [19].

Many of these models are developed analytically by linearizing a turbine model at a particular operating point using blade element momentum (BEM) theory to determine aerodynamic loads and the method of assumed modes [20] to model turbine flexure. Another method is to model the turbine as a system of rigid bodies with flexible linkages [21] (an approach that may also use BEM for aerodynamic loads). More on the modeling of wind turbines can be found in [22].

Here, we take advantage of a nonlinear model implemented in the FAST code [23] that utilizes Kane's method [24] to numerically simulate the kinematics of a turbine model based on assumed modes and BEM theory

with aerodynamic loads calculated by AeroDyn [25]. FAST simulates the turbine in constant (and possibly non-uniform) wind conditions to find a solution that changes only as a function of rotor position and then computes a linearized model by calculating the coefficients describing the perturbation of the system configuration/state with respect to a set of specified input perturbations.

Linearization commonly renders a kinematic system of the form

$$M(\theta) \cdot \Delta \ddot{q} + C(\theta) \cdot \Delta \dot{q} + K(\theta) \cdot \Delta q$$
$$= F(\theta) \cdot \Delta u + F_d(\theta) \cdot \Delta v_d \quad (1)$$

where the $M(\theta)$, $C(\theta)$, $K(\theta)$, $F(\theta)$, and $F_d(\theta)$ coefficients are dependent on the operating point and can be parameterized by the rotor azimuth position θ. The vector of configuration variables Δq represents deviation of the turbine away from the nominal operating point (at each rotor position).

The most complex turbine model we use in this paper includes a single generator degree of freedom (DOF), a flexible drive train mode, and a flap mode for each of three blades. FAST supports up to 24 degrees of freedom for a 3-bladed turbine. The vector Δu represents deviations of blade pitch(es) and/or generator torque from their nominal levels, and Δv_d represents deviations in hub height wind speed (that occur uniformly across the rotor plane).

The system (1) can be manipulated into state-space form:

$$\dot{x} = A(\theta) \cdot x + B(\theta) \cdot u + B_d(\theta) \cdot v_d$$
$$y = C(\theta) \cdot x + D(\theta) \cdot u + D_d(\theta) \cdot v_d \quad (2)$$

where $x = \begin{bmatrix} \Delta q^T \Delta \dot{q}^T \end{bmatrix}^T$ represents the deviation in position or velocity of the configuration variables. The output vector y may contain any quantity that can be determined from the system state; we keep track of perturbations in the high-
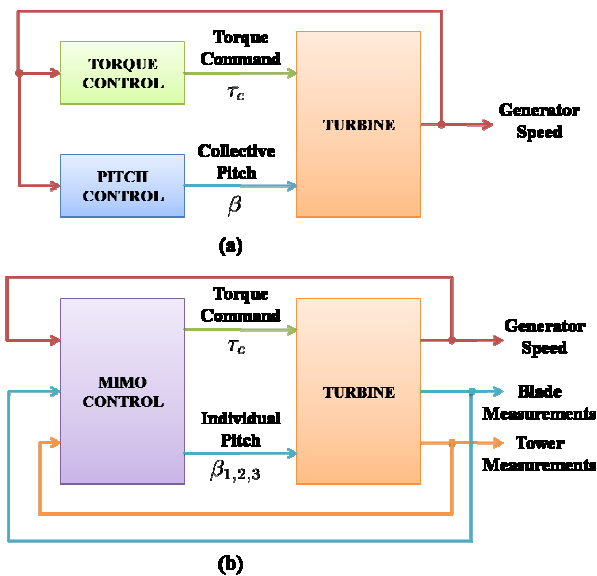
Fig. 2. (a) Traditional turbine control is based on generator speed feedback alone. Torque and pitch controllers are treated as separate SISO loops. (b) MIMO control is a hallmark of the controllers in ongoing research; the controller has access to individual blade measurements in addition to generator speed and may also utilize measurements of tower motion and strain.

speed shaft velocity and the flap (out of rotor-plane) bending moment of each blade. Since all variables represent perturbations away from their nominal values, we drop the Δ for notational simplicity. The coefficient matrices in (1)-(2), for any particular operating point in constant (but not necessarily uniform) wind conditions, are obtained from the numerical linearization provided by FAST.

We evaluate a turbine model based on the 600kW, 3-bladed, upwind, variable-speed, horizontal-axis Controls Advanced Research Turbine (CART3) located at the National Renewable Energy Laboratory (NREL). The CART3 has a rated rotor speed of 41.7 revolutions per minute (rpm); the velocity of the low-speed shaft (connected to the rotor) is stepped up by a gear box so that the high-speed shaft and generator run at a rated speed of 1800 rpm.

Changes in the linearized turbine model occur with operating point (total wind speed v, rotor speed ω, and blade pitch β) as the turbine operates in different regions. These regions can generally be described as follows [2]:

- In Region 1, the wind speed is too low to warrant turbine startup. The blades are pitched at full feather (the pitch angle that generates minimum aerodynamic torque). Once the wind speed is large enough (above 5 m/s for the CART3) for machine start-up, the blades are pitched to the normal Region 2 angle. At nominal pitch, the aerodynamic lift is in a direction to produce torque and accelerate the rotor. Once generator speed reaches 430 rpm for the CART3, generator torque is turned on and the turbine begins power production in Region 2.
- In Region 2, the wind speed and the generator torque are below "rated." Blade pitch is held constant at the optimal value β_* that gives maximum aerodynamic torque. Each wind speed has a corresponding rotor speed at which the

greatest possible aerodynamic torque τ_a is generated. It turns out that when the blade pitch is held at the optimal β_*, there is a constant value λ_*, or tip speed ratio (TSR) $\lambda = R \cdot \omega/v$, (where R is blade radius) that maximizes aerodynamic torque τ_a. Normally a function of TSR and pitch, the fraction $C_p(\lambda, \beta_*)$ of aerodynamic power obtained from the total wind power is a maximum when $\lambda = \lambda_*$. So, the control objective in Region 2 is to command torque so that ω tracks with v and gives a TSR of λ_*.

- In Region 2½, the wind speeds are approaching those that provide rated power. This is a transition region where the torque command is commonly computed as an affine function of generator speed such that rated torque is reached before the rated generator speed.
- In Region 3, the wind speed is at or above (11.7 m/s for the CART3) that which will generate rated power. The generator torque is held constant at rated, and blade-pitch control is used to limit aerodynamic power by regulating turbine speed at the rated speed. Advanced controls are also designed to mitigate loads on the blades and tower.

With a set of state-space descriptions from FAST, we explore how the linearized models vary with operating point by evaluating the frequency response of the system at various points. First, we use FAST to linearize the turbine at each of 36 rotor positions while the turbine operates at an average speed of 41.7 rpm and a constant blade pitch of 12.6 deg, but with different wind profiles. Two sets of linearizations are obtained in time-constant wind conditions, in line with the nacelle and having average speed of 18m/sec over the plane of the rotor. However, for one set of linearizations the wind conditions are uniform and for the second set the wind has vertical shear so that the horizontal wind speed at the bottom of the rotor differs from that at the top by 40%.

The frequency responses of perturbations in the generator high-speed shaft velocity (HSSV) and flap bending moment at the root of the blades are computed for pitch perturbations made collectively on all blades. This computation is done for the linearized model at each azimuth position. Fig. 3 shows the envelope of magnitude responses obtained by finding the minimum and maximum gain at each frequency over all responses. The top plot depicts HSSV response and the bottom plot depicts bending moment response. Blue solid lines denote the envelope from models obtained in the presence of shear and green solid lines denote the envelope obtained from models in uniform conditions. A "mean" model representing the turbine over all azimuth angles is obtained by computing the average of each of the coefficient matrices in (2). In Fig. 3 the response of the mean models are denoted by dashed red and magenta lines for shear and uniform conditions, respectively.

Fig. 3 shows that there is a small amount of variation in the bending moment response and essentially no variation in the HSSV response. The minimal variation observed in the responses suggests that the mean model (averaged across all
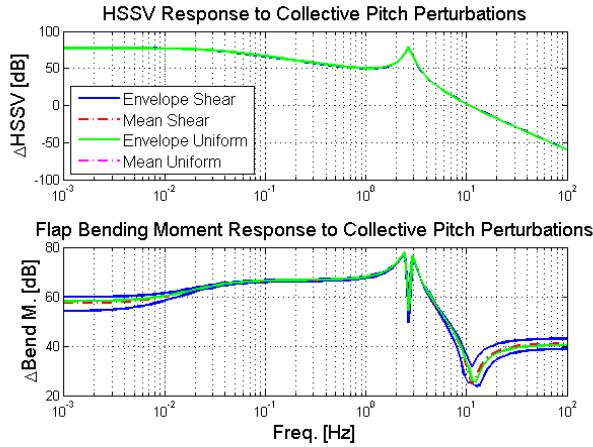
Fig. 3. Study of turbine linear model dependence on rotor azimuth position: both plots show minimum and maximum (envelope) responses observed due to collective pitch perturbations over all rotor positions as well as the averaged state-space response. High-speed shaft velocity (HSSV) response to pitch (top plot) is highly independent of rotor position, while the blade bending moment (bottom plot) shows some azimuth dependence when shear is present.

rotor positions) might suffice as a basis for control design, and that is the approach we take here.

Next, we investigate variation in the mean models for a wider range of operating points in terms of the HSSV response to perturbations in pitch and torque, but in uniform wind conditions. Fig. 4 depicts the envelopes obtained from the averaged models for generator speeds below rated (Region 2) and at rated (Region 3) for various levels of wind speed (uniform with no shear). In Region 2 where speed is regulated via generator torque, there is a fair amount of variance in the turbine response. The two envelopes in Fig. 4 for Region 2 operation show the response in HSSV due to perturbations in generator torque and blade pitch, respectively.

Additionally, there are two envelopes displayed in Fig. 4 for Region 3 operation. One envelope is for operating points at different wind speeds with pitch set to maintain rotor speed at rated and the other is for various pitch angles with a wind speed of 18 m/sec as might occur during transient pitch response. In Region 3 where, in modern utility scale turbines, speed is regulated by adjusting blade pitch angle, less variance is observed in the averaged, linear models across expected operating points. This suggests that a single controller might suffice when operating at rated power.

III. STANDARD WIND TURBINE CONTROL

A. Region 2 Control

In Region 2, the generator torque τ_c that achieves λ_* is obtained as a function of rotor speed:

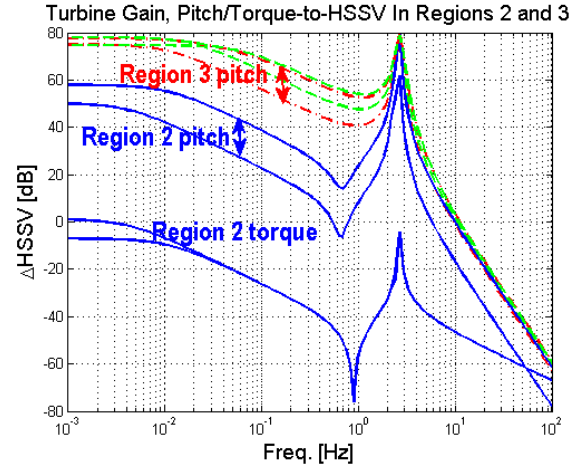$$\tau_c = K \cdot \omega^2 \tag{3}$$

Fig. 4. Perturbations in HSSV response for different operating regions and wind speeds. The lower two envelopes (solid blue) show the changes in response to torque and pitch perturbations across a range of Region 2 wind speeds (5–13m/s). The two upper envelopes (dashed red and green) show the change in response to pitch perturbation across various Region 3 operating points. There is a large variance in HSSV response to turbine pitch throughout Region 2 (5–13m/s). In Region 3, where pitch is adjusted to maintain a rotor speed of 41.7 rpm, HSSV response varies less, both with varying wind speed (green, 16–24 m/s) and with pitch (red, 4–18 deg, wind speed = 18 m/s).

where the gain is

$$K = \frac{1}{2} \rho \pi R^5 \frac{C_{p_{max}}}{\lambda_*^3}, \tag{4}$$

ρ is the air density, and C_{pmax} is the optimal power coefficient ($=C_p(\lambda_*,\beta_*)$). By convention, positive τ_c is in a direction that decelerates the rotor; that is, (3) is a restorative torque and can be shown to render a stable closed-loop system [2]. As wind speed changes, the rotor is accelerated due to the difference in aerodynamic and generator torque. Adjusting generator torque according to (3) causes the rotor speed to settle correctly so that in constant wind conditions, λ_* is achieved. This control law (one that is static and determined by absolute speed rather than speed perturbation) may be augmented with additional dynamic compensation to alleviate loads [26].

B. Region 3 Control

Referring to Fig. 1, generator speed is measured and passed to both the torque and pitch controllers. Classical proportional-integral-derivative (PID) control techniques are typically used to design the blade pitch controller for Region 3 [19] to regulate turbine speed in the presence of varying wind conditions. In this case, the perturbations $\Delta\theta$ to the nominal pitch are computed as

$$\Delta\theta(s) = \left[K_P + \frac{K_I}{s} + \frac{K_D \cdot s}{s \cdot \tau + 1} \right] \Delta\omega(s) \tag{5}$$
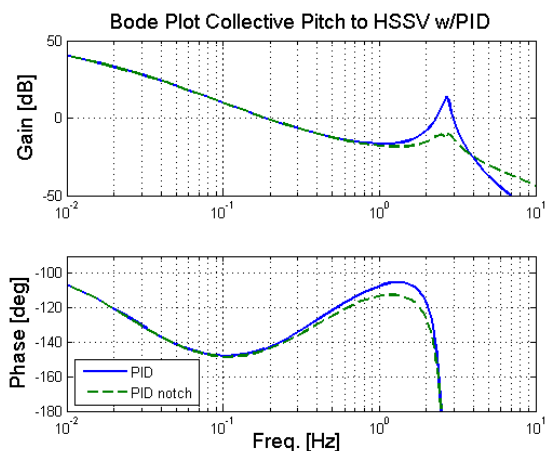
Fig. 5. PID controllers often benefit from the use of additional notch compensation to damp known resonances.

where $\Delta\omega$ is the generator or rotor rotational speed error. Using only rotor speed error as feedback, the pitch command $\Delta\theta$ is necessarily collective (the same for all blades). The K_p, K_I, and K_D gains are chosen to give "desired" closed-loop characteristics. Further discussions on methods for choosing these gains are found in [27,28]. Often, the standard PID control is augmented (multiplied) with notch transfer functions to add damping to known resonances.

An example of the use of PID with notch filtering would be to damp out the drive train resonance clearly visible at 2.8 Hz in Figs. 3 and 4. The loop gain for a PID controller in series with a Region 3, linearized model is shown in Fig. 5. The notch provides attenuation of the resonance so that the loop crossover can be placed at 0.2 Hz while retaining more than 10 dB of gain margin at higher frequencies. The time response of this controller to various wind disturbances can be observed (along with more advanced controllers) in Fig. 7—see Section IV-C for associated details.

IV. ADVANCED CONTROL

A. Advanced Region 2 Control

Much of the advanced control research is logically divided between optimization of power capture in Region 2 and load mitigation in Region 3. In Region 2, research is further divided between investigations that incorporate detailed models of the generator electromechanical system and power electronics and those that view the generator torque in terms of a static gain (as in the previous section) that responds instantly to commanded torque. Where studies involve electromechanical models, advanced research congregates around maximum power point tracking (MPPT) and sliding mode approaches [16-18] or extremum seeking control [29]. Many of the MPPT and extremum seeking approaches can be considered nonlinear, but they may begin design with at least some form of linearization. In contrast, the techniques in [13-15] and references therein, incorporate

the non-linear relationship between aero-dynamic torque, pitch, and wind speed.

A common theme seems to account for the nonlinear dependence of $C_p(\lambda, \beta)$ on its parameters, but not structural nonlinearity. The study in [15] is apparently one of the few that designs for both generator/electromechanical dynamics and the linearized, flexible turbine structure. Additionally, adaptive approaches for maximizing power capture are studied in [11-13]. Controls for structural load mitigation (typically absent in studies on power capture) has also been developed for use in Region 2. In simulation [26], these controllers have been shown to reduce blade loading by 24%. In [30], load mitigating Region 2 controllers were designed and tested on an actual turbine (CART2, a 2-bladed turbine similar to CART3) and shown to significantly reduce tower loads.

B. Advanced Region 3 Control

Time invariant, MIMO methods [3,4,7] tend to be the most prevalent in the research of advanced controls for Region 3, but adaptive [9,10] and novel gain-scheduling [31] approaches are also investigated. Since even under constant wind conditions, the turbine has time-varying, periodic (with each rotation of the rotor) dynamics, work has been done on the use of periodic control [32,33] and multi-blade coordinate (MBC) based control [8,34,35]. In [34], under non-extreme conditions, MBC and periodic control are found to be very comparable and time-invariant control is not far behind.

C. An Example LTI, MIMO, Region 3 Controller

Nearly all of these advanced MIMO methods are state-space based rather than transfer-function based. State-space control techniques lend themselves nicely to MIMO systems, extend naturally to time-varying and periodic control applications, and commonly utilize an observer to estimate system states. These techniques also incorporate models of the wind, either by augmenting the observer with a model of a persistent wind disturbance as in Fig. 6(a), or indirectly in an output referred sense by augmenting the plant model with dynamics as in Fig. 6(b). The PID controller from the previous section can be viewed in terms of Fig. 6(b); a (persistent, output referred) step disturbance is modeled by the integrator and the proportional, derivative, and notch functions are implemented in the controller $K(s)$. In both of these diagrams the output y may consist of generator, blade, and tower measurements, while the control u may include torque and individual pitch commands.

When observer augmentation, often referred to as disturbance accommodating control (DAC), is feasible, there can be asymptotically perfect reconstruction of the modeled disturbance in the observer ($v_d - \hat{v}_d \to 0$). Then, with an additional matching condition [7], it is possible to cancel out the effect of this disturbance on the output y perfectly through correct selection of the gain K_V.

With plant augmentation, the intuitive and explicit interpretation of the disturbance model as being
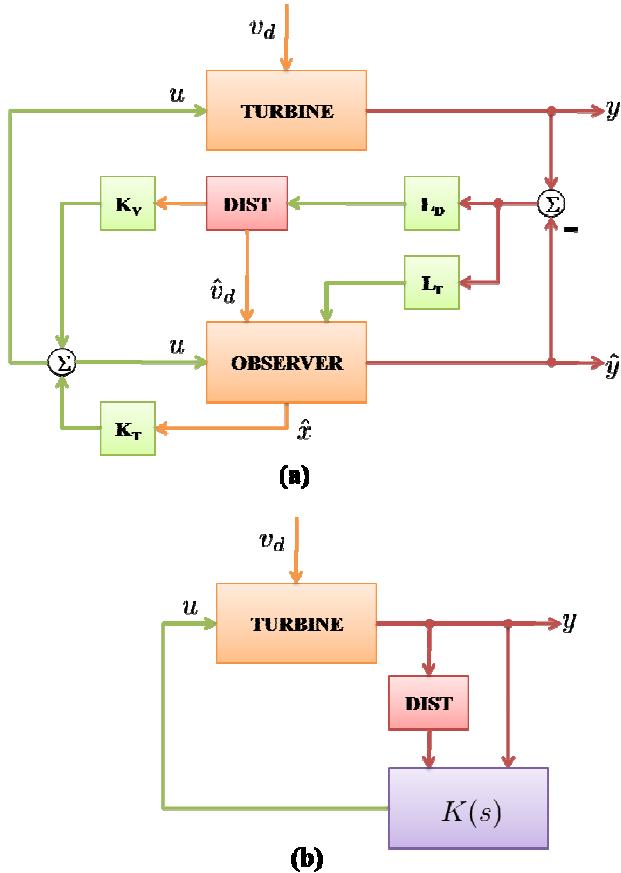
(a)

(b)

Fig. 6. Two common architectures for including models of persistent disturbances. (a) In disturbance accommodating control, the disturbance dynamics are observable from the plant outputs and can be estimated in the observer. (b) In plant augmentation, the plant output is augmented with a model of the disturbance that is output referred.
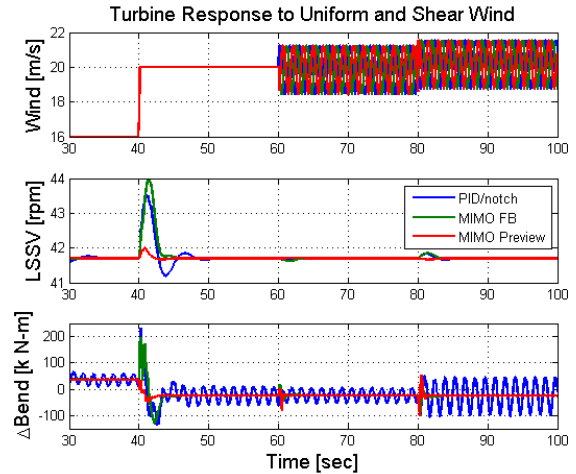

Fig. 7. Turbine response using three different controllers. Wind (top) starts out uniform with a step change at 40sec. Shear is introduced at 60 seconds so the difference in wind experienced by each blade is visible in the wind plot. Low speed shaft velocity (center) is regulated with 0 DC error since all three controllers have integral control on speed error. Only the MIMO controllers reject the 1P variations in bending moment (bottom) since they have access to those measurements and incorporate models of 1P disturbances.

representative of certain types of wind disturbances v_d acting on the turbine is lost. Instead, undesirable, but expected, behaviors in the measured outputs (offsets, once per revolution (1P) oscillations) determine the disturbance model used. In lieu of an intuitive connection with exogenous disturbances, plant augmentation always provides perfect asymptotic rejection of the disturbance at the measured output.

Assuming measurements of HSSV error and blade root bending moments are available, we design a (Region 3) controller using a wind turbine model linearized in uniform, 18 m/sec wind, at a nominal pitch of 12.6 deg, and rated rotor speed of 41.7 rpm. We take the approach in Fig. 6(b) and feed the HSSV speed error to an integrator to reject DC speed errors and feed each bending moment measurement into separate disturbance models each with transfer function

$$D_{1P}(s) = \frac{\omega_{1p}^2}{s^2 + \omega_{1P}^2}. \qquad (6)$$

This guarantees that 1P variations in bending moment can be rejected independently at each blade. A stabilizing controller $K(s)$ is then designed for the augmented plant

[36]. In implementation, the disturbance models are subsumed into the controller. Often, a majority of the 1P variation in the blade dynamics is the same for each blade, but simply shifted by multiples of 1/3 of a revolution. In this case, designing in a MBC framework can accomplish similar rejection with a significant reduction in controller complexity (three 2$^{\text{nd}}$-order $D_{1P}(s)$ systems are replaced by a single integrator) [34].

Our resulting (non-MBC) controller is simulated with the full non-linear model of the CART3 provided by FAST. As shown in Fig. 7, the closed-loop turbine is subjected to a wind that has a uniform (across the rotor plane) step change of from 16m/s to 20m/s. Starting at 60 sec shear is introduced so that the turbine is subjected to two non-uniform wind profiles that can be observed in the top plot of Fig. 7 which shows the wind speed at each blade. The non-uniform profile starts when a 10% shear, both vertical and horizontal, is first introduced at 60 sec and then changes when there is a reversal in polarity of both vertical and horizontal shear at 80 sec. The PID/notch controller (blue) does an excellent job regulating rotor speed (LSSV), but does nothing to mitigate the 1P variation in bending moment. The MIMO, plant augmented controller (green) accomplishes both speed regulation and mitigation of the blade root loads. Only the response of blade 1 is shown in Fig. 7 since the response of the other is similar. However, if the dynamics were unique for each blade, this controller would still accomplish perfect asymptotic rejection of 1P variations. The preview controller (red) also displayed in Fig. 7 is explained in the next section.

V. New Control Strategies Enabled by Novel Wind Measurement Techniques

Currently, most control algorithms depend on measurements from turbine structure and drive train for use in the control feedback. Often these turbine measurements are unreliable or exhibit delayed response to disturbances acting on the turbine. This constrains the controls to react to complex atmospheric disturbances after their effects have been "felt" by the turbine. Thus, there is an inherent lag between the time that a disturbance arrives and the time that the control actuator begins to mitigate resulting loads. A considerable advantage in load mitigating capability can be attained by measuring atmospheric phenomena upwind of the turbine before they impact the turbine rotor. The needed control actuation signals can then be prepared in advance and applied as the inflow to the turbine changes with potentially significant load mitigation improvement.

New lidar technologies are capable of measuring velocity upwind of the turbine with sample rates in the 10's of Hz [37]. With these measurements, it is possible to design preview controllers as depicted in Fig. 8 that can adjust pitch (and/or torque) as necessary before wind disturbances arrive at the turbine. The preview control can be designed in unison with the feedback control [36] as depicted in Fig. 9(a) or separately from feedback [38] as in Fig. 9(b).

A plant augmented, preview controller is designed with the same techniques as used in the design of the MIMO controller of the previous section. As explained in [36], the generalized plant approach extends so that a combined feedback and feedforward (preview) controller can be designed. The response of the resulting preview controller is displayed along with that of the PID/notch and MIMO, feedback controllers in Fig. 7. As expected, the preview controller significantly improves performance without large increases in actuation.

VI. Summary and Ongoing and Future Challenges

Proper characterization of the wind inflow to a turbine is important for improved turbine design. Concentrated wind gusts, rapid wind direction changes, or passage of energetic atmospheric structures impose critical loads on individual wind turbines and blades [39]. These extreme events decrease turbine lifetimes, cause component failures, and can even threaten catastrophic machine failure. It is crucial to understand the complex wind inflow to the turbine in order to design load mitigating controls which adequately account for these complex atmospheric phenomena.

Preliminary investigation of preview, feedforward techniques indicate the promise of tantalizingly large improvements in controller performance. Implementation of such methods relies heavily on new measurement technologies that each come with their own, characteristic distortion and noise issues [39]. Even if these prove to be surmountable, there remains the fact that an upstream, wind, velocity profile will hardly be the same when it arrives at the turbine. Modeling the stochastic nature of the change in wind profile as it travels and optimizing feedforward control
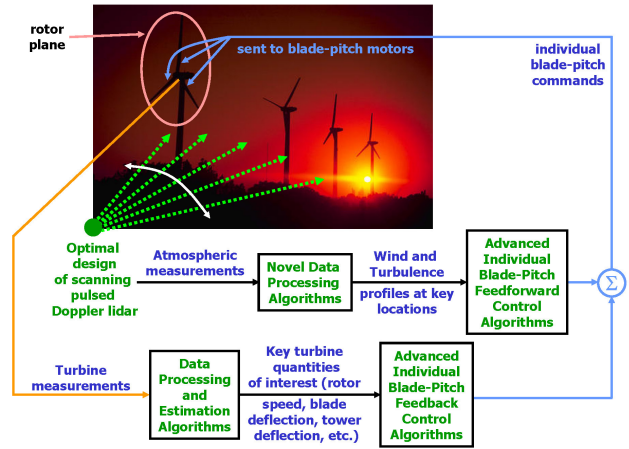

Fig. 8. Availability of lidar measurements enables the implementation of disturbance feedforward methods.
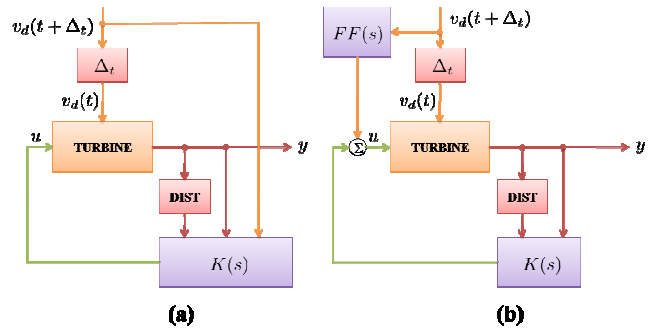

Fig. 9. Preview control uses "look-ahead" measurements of incoming wind disturbances to generate pre-actuation. (a) Compensation designed in conjunction with feedback control. (b) Stand-alone, feedforward control based on plant inversion.

for operation in the presence of the resulting measurement errors will be pivotal in realizing the anticipated performance improvement from preview control.

Pitch actuation in utility scale turbines is inherently rate limited and this is one of the reasons pre-actuation can provide such large performance gains. In a previous study [40], excessively high pitch rates were required to obtain similar performance improvements using feedforward without preview techniques. This pitch related limitation may be circumvented with new actuation technologies currently being investigated. These include such devices as trailing edge flaps, micro-tabs, adaptive trailing edge devices, etc. [41,42]. New sensors being investigated include localized flow-measuring devices (such as pitot tubes), embedded fiber optic sensors, etc. The goal is to develop "smart" rotor blades with embedded sensors and actuators that provide for blade-local control of aerodynamic effects. The challenges to this new technology include developing new actuators and sensors that are maintenance free, do not require significant extra weight and cost, and are reliable and effective for blade fatigue load mitigation.

In this paper we reviewed regions of wind turbine operation and their associated control objectives. The focus was on methods for speed regulation and structural load mitigation, but the reader interested in other areas will find

the references a good starting point. We demonstrated methods for pitch control, both standard and advanced, some of which show great potential for improved performance. In conclusion we have touched on further work which may be pivotal in realizing the improvements that recent research suggests is possible with advanced control methods.

REFERENCES

[1] World Wind Energy Association, http://www.wwindea.org/.

[2] L. Y. Pao and K. E. Johnson, "A Tutorial on the Dynamics and Control of Wind Turbines and Wind Farms," *Proc. Amer. Ctrl. Conf.*, June 2009.

[3] P. Caselitz, W. Kleinkauf, T. Kruger, J. Petschenka, M. Reichardt, and K. Storzel, "Reduction of Fatigue Loads on Wind Energy Converters by Advanced Control Methods," *Proc. Euro. Wind Energy Conf.*, pp. 555–558, Oct. 1997.

[4] M. J. Balas, Y. J. Lee, and L. Kendall, "Disturbance Tracking Control Theory with Application to Horizontal Axis Wind Turbines," *Proc. AIAA/ASME Wind Energy Symp.*, pp. 95–99, Jan. 1998.

[5] E. A. Bossanyi, "The Design of Closed Loop Controllers for Wind Turbines," *Wind Energy*, 3: 149–163, 2000.

[6] N. A. Cutululis, E. Ceanga, A.D. Hansen, and P. Sørensen, "Robust Multi-Model Control of an Autonomous Wind Power System," *Wind Energy*, 9: 399–419, 2006.

[7] A. D. Wright, "Modern Control Design for Flexible Wind Turbines," NREL Report No. TP-500-35816, National Renewable Energy Laboratory, 2004.

[8] M. Geyler and P. Caselitz, "Robust Multivariable Pitch Design for Load Reduction on Large Wind Turbines," *J. Solar Energy Eng.*, 130(3): 031014-1 – 031014-12, Aug. 2008.

[9] J. B. Freeman and M. J. Balas, "An Investigation of Variable-Speed Horizontal-Axis Wind Turbines Using Direct Model-Reference Adaptive Control," *Proc. AIAA/ASME Wind Energy Symp.*, pp. 66–76, Jan. 1999.

[10] S. A. Frost, M. J. Balas, and A. D. Wright, "Direct Adaptive Control of a Utility-Scale Wind Turbine for Speed Regulation," *Int. J. Robust Nonlinear Ctrl.*, 19(1): 59–71, Jan. 2009.

[11] K. E. Johnson, L. Y. Pao, M. J. Balas, V. Kulkami, and L.J. Fingersh, "Stability Analysis of an Adaptive Torque Controller for Variable Speed Wind Turbines," *Proc. IEEE Conf. Decision and Ctrl.*, pp. 4087–4094, Dec. 2004.

[12] K. E. Johnson and L. J. Fingersh, "Adaptive Pitch Control of Variable-Speed Wind Turbines," *J. Solar Energy Eng.*, 130(3): 031012-1 – 031012-7, Aug. 2008.

[13] Y. D. song, B. Dhinakaran, and X. Y. Bao, "Variable Speed Control of Wind Turbines using Non-Linear and Adaptive Algorithms", *J. Wind Eng. and Ind. Aerodynamics*, 85(3): 293–308, April 2000.

[14] B. Boukhezzar, H. Siguerdidjane, and M. M. Hand, "Nonlinear Control of Variable-Speed Wind Turbines for Generator Torque Limiting and Power Optimization," *J. Solar Energy Eng.*, 128(4): 516–530, Nov. 2006.

[15] A. Kumar and K. Stol, "Simulating MIMO Feedback Linearization Control of Wind Turbines Using FAST," *Proc. AIAA/ASME Wind Energy Symp.*, Jan. 2008.

[16] J. Yaoqin, Y. Zhongging, and C. Binggang, "A New Maximum Power Point Tracking Control Scheme for Wind Generation," *Proc. IEEE Int. Conf. Power Sys. Tech.*, pp. 144–148, Oct. 2002.

[17] E. Koutroulis and K. Kalaitzakis, "Design of a Maximum Power Tracking System for Wind-Energy Conversion Applications," *IEEE Trans. Ind. Electronics*, 53(2): 386–394, April 2006.

[18] T. Pan, Z. Ji, and Z. Jiang, "Maximum Power Power Point Tracking of Wind Energy Conversion Systems Based on Sliding Mode Extremum Seeking Control," *Proc. IEEE Energy Conf.*, pp. 1–5, Nov. 2008.

[19] A. D. Wright and L. J. Fingersh, "Advanced Control Design for Wind Turbines Part I: Control Design, Implementation, and Initial Tests," NREL Report No. TP-500-42437, National Renewable Energy Laboratory, March 2008.

[20] S. Suryanarayanan and A. Dixit, "On the Dynamics of the Pitch Control Loop in Horizontal Axis Large Wind Turbines," *Proc. Amer. Ctrl. Conf.*, pp. 686–690, June 2005.

[21] K. A. Stol and G. S. Bir, "SymDyn User's Guide," NREL Report No. EL-500-33845, National Renewable Energy Laboratory, 2003.

[22] P. Moriarty and C. P. Butterfield, "Wind Turbine Modeling Overview for Control Engineers," *Proc. Amer. Ctrl. Conf.*, June 2009.

[23] J. M. Jonkman and M. L. Buhl, "FAST User's Guide," NREL Report No. EL-500-38230, National Renewable Energy Laboratory, 2005.

[24] T. R. Kane and D. A. Levinson, *Dynamics: Theory and Applications,* McGraw-Hill, 1985.

[25] A. C. Hansen, *User's Guide to the Wind Turbine Dynamics Computer Programs YawDyn and AeroDyn for ADAMS version 11.0*, Mech. Eng. Dept., Univ. of Utah, 1998.

[26] K. Stol, "Disturbance Tracking Control and Blade Load Mitigation for Variable-Speed Wind Turbines," *J. Solar Energy Eng.*, 125(4): 396–401, Nov. 2003.

[27] T. Burton, D. Sharpe, N. Jenkins, and E. Bossanyi, *Wind Energy Handbook*, John Wiley & Sons, New York, NY, pp. 488–489, 2001.

[28] Maureen Hand, "Variable-Speed Wind Turbine Controller Systematic Design Methodology: A Comparison of Non-Linear and Linear Model-Based Designs," NREL Report No. TP-500-25540, National Renewable Energy Laboratory, July 1999.

[29] M. Komatsu, H. Miyamoto, H. Ohmori, and A. Sano, "Output Maximization Control of Wind Turbine Based on Extremum Control Strategy," *Proc. Amer. Ctrl. Conf.*, pp. 1739–1740, June 2001.

[30] A. D. Wright, L. J. Fingersh, and K. A. Stol, "Design and Testing Controls to Mitigate Tower Dynamic Loads in the Controls Advanced Research Turbine," National Renewable Energy Laboratory, NREL/CP-500-40932, Golden, CO, 2007.

[31] A. Kumar and K. Stol, "Scheduled Model Predictive Control of a Wind Turbine," *Proc. AIAA/ASME Wind Energy Symp.*, Jan. 2009.

[32] K. Stol and M. Balas, "Full-State Feedback Control of a Variable-Speed Wind Turbine: A Comparison of Periodic and Constant Gains," *J. Solar Energy Eng.*, 123(4): 319–326, Nov. 2001.

[33] K. Stol and M. Balas, "Periodic Disturbance Accommodating Control for Speed Regulation of Wind Turbines," *Proc. AIAA/ASME Wind Energy Symp.*, pp. 310–320, Jan. 2002

[34] K. Stol, H. G. Moll, and G. Bir, "A Comparison of Multi-Blade Coordinate Transformation and Direct Periodic Techniques for Wind Turbine Control Design," *Proc. AIAA/ASME Wind Energy Symp,*. Jan. 2009.

[35] G. Bir, "Multi-Blade Coordinate Transformation and its Application to Wind Turbine Analysis," *Proc. AIAA/ASME Wind Energy Symp.*, Jan. 2008.

[36] J.C. Doyle, K. Glover, P.P. Khargonekar, and B.A. Francis, "State-space Solutions to Standard H_2 and H_∞ Control Problems," *IEEE Trans. Automatic Control*, 34(8): 831-847, Aug. 1989.

[37] M. Harris, M. Hand, and A. Wright. Lidar for turbine control. NREL Technical Report, NREL/TP-500-39154, 2006.

[38] B. P. Rigney, L. Y. Pao, and D. A. Lawrence, "Nonminimum Phase Dynamic Inversion for Settle Time Applications," *IEEE Trans. Ctrl. Sys. Tech.*, Vol. 17, 2009.

[39] N. D. Kelley, B. J. Jonkman, G. N. Scott, and Y. L. Pichugina, "Comparing Pulsed Doppler LIDAR with SODAR and Direct Measurements for Wind Assessment," NREL Report No. CP-500-41792, National Renewable Energy Laboratory, July 2007.

[40] J. H. Laks, L. Y. Pao, and A. Wright, "Combined Feedforward/Feedback Control of Wind Turbines to Reduce Blade Flap Bending Moments," *Proc. AIAA/ASME Wind Energy Symp.*, Jan. 2009.

[41] International Energy Agency (IEA), "The Application of Smart Structures for Large Wind Turbine Rotor Blades," *Proc. IEA Topical Expert Meeting*, May 2008.

[42] M. Lackner and G. van Kuik, "A Comparison of Smart Rotor Control Approaches Using Trailing Edge Flaps and Individual Pitch Control," *Proc. AIAA/ASME Wind Energy Symp.*, Jan. 2009.